Acta Crystallographica Section D
Biological Crystallography
ISSN 0907-4449

Crystallization and preliminary X-ray diffraction data of an archaeal asparagine synthetase related to asparaginyl-tRNA synthetase

Christophe Charron,‡ Hervé Roy, Mickaël Blaise, Richard Giegé* and Daniel Kern

Département 'Mécanismes et Macromolécules de la Synthèse Protéique et Cristallogenèse', UPR 9002, Institut de Biologie Moléculaire et Cellulaire du CNRS, 15 Rue René Descartes, F-67084 Strasbourg CEDEX, France

‡ Present address: Laboratoire de Cristallographie et Modélisation des Matériaux Minéraux et Biologiques, UMR 7036 CNRS-UHP, Groupe Biocristallographie, Faculté des Sciences et Techniques, BP 239, 54506 Vandoeuvre-lès-Nancy, France.

Correspondence e-mail: r.giege@ibmc.u-strasbg.fr

Received 22 December 2003
Accepted 6 February 2004

The archaebacterial-type asparagine synthetase A from *Pyrococcus abyssi* (AS-AR), which is related to asparaginyl-tRNA synthetase, was crystallized in two different conditions using the hanging-drop vapour-diffusion method. Crystals belonging to space group $C2$ with unit-cell parameters a = 103.6, b = 43.3, c = 121.5 Å, β = 112.6° and one dimer per asymmetric unit were obtained in the presence of 2-propanol and PEG 4000 at pH 5.6. Another crystal form was obtained in the presence of dioxan and belongs to the monoclinic space group $P2_1$, with unit-cell parameters a = 96.8, b = 103.9, c = 98.4 Å, β = 107.5° and two dimers per asymmetric unit. Two different native diffraction data sets were collected to 2.3 and 3.0 Å resolution using synchrotron radiation and cryocooling for crystals belonging to space groups $C2$ and $P2_1$, respectively.

1. Introduction

Analysis of complete archaeal genomes reveals that all archaea that possess asparaginyl-tRNA synthetases (AsnRS) also display a second ORF encoding its counterpart truncated from the anticodon-binding domain, initially named AsnRS2. Analysis of the functional properties of AsnRS2 from *Pyrococcus abyssi* have shown that this enzyme, in contrast to AsnRS, does not sustain asparaginyl-tRNA^{Asn} synthesis, but is instead capable of converting free aspartic acid (Asp) into asparagine (Asn). It generates Asn by the amidation of the β-COOH of Asp, which is activated by ATP in the presence of free ammonia as an amide-group donor (Roy *et al.*, 2003). This archaeal enzyme is distinct from the tRNA-dependent amidotransferase that converts Asp-tRNA^{Asp} to Asn-tRNA^{Asn} (Becker & Kern, 1998), but is a homologue of the bacterial ammonia-dependent asparagine synthetase A (AS-A) and is thus called archaebacterial asparagine synthetase A (AS-AR). It differs from the asparagine synthetases B (AS-B) found in all eukaryotes and in most prokaryotes (Scofield *et al.*, 1990), the enzymes that produce Asn by amidation of Asp in the presence of glutamine (Gln) as an amide-group donor.

The three-dimensional structures of AS-A from *Escherichia coli* and the catalytic domain of aspartyl-tRNA synthetase (AspRS) from yeast show similar topologies. The three consensus motifs that are specific for the active site of class II aminoacyl-tRNA synthetases (which AspRS belongs to) are also found in AS-A (Nakatsu *et al.*, 1998). However, in spite of this overall structural similarity, AspRS activates the α-COOH of Asp before transferring it to the tRNA, while AS-A activates the β-COOH of Asp before it reacts with ammonia.

The phylogenetic tree reconstructed by alignment of AS-AR with AspRS and AsnRS sequences shows that AsnRSs and AS-ARs are derived from an archaeal AspRS ancestor (Roy *et al.*, 2003). The fact that AsnRS is present in the three phylae while AS-AR is archaeal-specific suggests that AsnRS appeared just before the split of the archaea and eukaryotes and AS-AR appeared after this split. The AS-AR gene was subsequently transferred into bacteria by lateral gene transfer, where it underwent structural changes, producing AS-A. Therefore, AS-ARs, which show ~40% sequence similarity to archaeal AspRSs, constitute the link in the evolutionary path between AspRS and eubacterial AS-A that led to the emergence of ammonia-dependent Asn synthesis.

The determination of the three-dimensional structure of AS-AR from *P. abyssi* will allow comparison of its active site with that of archaeal AspRS. It will also constitute a significant contribution to the understanding of the different evolutionary origins of the activation mechanisms of the α-COOH and β-COOH groups of Asp. In turn, this will help in understanding on a molecular basis how nature substituted the ancestral biosynthetic pathway of Asn formation from Asp bound to tRNA^{Asn} by a direct amidation of free Asp.

We describe here the crystallization of the AS-AR from *P. abyssi* and the first analysis of X-ray diffraction data from the AS-AR crystals.

2. Materials and methods

2.1. Preparation of pure AS-AR from *P. abyssi*

AS-AR from *P. abyssi* was overexpressed in *E. coli* BL21 Codon+ RIL strain (Stratagen). Overproducing cells were grown at 310 K and harvested 10 h after induction of AS-AR biosynthesis by addition of 0.5 m*M* IPTG. 15 g biomass was suspended in 45 ml 100 m*M* Tris–HCl buffer pH 8.0 containing 5 m*M* β-mercaptoethanol, 0.5 m*M* EDTA and 1 m*M* AEBSF (a serine protease inhibitor provided by Uptima). 15 ml aliquots were sonicated and the lysates were centrifuged for 2 h at 105 000*g*. The supernatant was then heated for 30 min at 343 K and the flocculated proteins sedimented by 15 min centrifugation at 5000*g*. After dialysis against 20 m*M* potassium phosphate buffer pH 7.2, the proteins were adsorbed onto a DEAE-cellulose column and eluted with a linear gradient of potassium phosphate from 20 m*M* pH 7.2 to 250 m*M* pH 6.8. The active fractions eluting at 155 m*M* salt were dialyzed, adsorbed onto a HPLC hydroxyapatite column (CHT20, Bio-Rad) equilibrated with 10 m*M* potassium phosphate pH 6.8 and the proteins eluted with a linear gradient of 10–250 m*M* potassium phosphate pH 6.5. The active fractions eluted at 170 m*M* salt were dialyzed against 20 m*M* Tris–HCl buffer pH 7.5, adsorbed onto a UNO-Q6 (Bio-Rad) ion-exchange column and eluted with a linear gradient of 0–200 m*M* NaCl. The fraction with AS-AR activity eluted at 150 m*M* salt was dialysed against 20 m*M* Tris–HCl buffer pH 7.5 and concentrated to 10 mg ml^{-1} ($\varepsilon_{280\text{nm}}$ = 50 780 M^{-1} cm^{-1}) by centrifugation in a Vivaspin concentrator (Sartorius). This protocol yielded 60 mg of pure enzyme. Its purity and homogeneity were checked by activity assay and denaturing gel electrophoresis.

2.2. Crystallization

Initial crystallization conditions were searched by sparse-matrix screening (Jancarik & Kim, 1991) using the vapour-diffusion technique in hanging drops at 293 K. 4 µl drops were equilibrated over 1 ml reservoirs. A total of 296 conditions were covered using four screens (Hampton Research Screen I and II, Molecular Dimensions Ltd Structure Screens and Decode Genetics Wizard I and II Screens). For each condition, 2 µl AS-AR solution (10 mg ml^{-1}) was mixed with 2 µl reservoir solution.

Table 1
Statistics of X-ray data measurement for *P. abyssi* AS-AR crystals.

Values in parentheses correspond to the last resolution shell.

Space group	*C*2	$P2_1$
Unit-cell parameters		
a (Å)	103.6	96.8
b (Å)	43.3	103.9
c (Å)	121.5	98.4
β (°)	112.6	107.5
Z	4	2
Resolution range (Å)	30–2.3 (2.38–2.30)	30–3.0 (3.11–3.00)
No. unique reflections	21186	33914
R_{sym} (%)	5.5 (18.0)	9.0 (16.1)
Completeness (%)	95.7 (91.6)	90.3 (97.9)
$\langle I/\sigma(I)\rangle$	17.4 (5.7)	8.9 (3.6)
Multiplicity	2.6	3.2

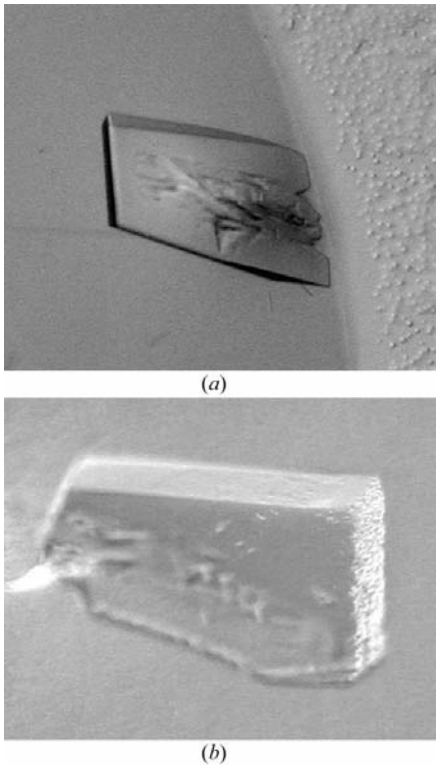

Figure 1
Crystals of AS-AR from *P. abyssi* in space group $P2_1$ (*a*), crystal dimensions 0.2 × 0.1 × 0.02 mm, and in space group *C*2 (*b*), crystal dimensions 0.3 × 0.15 × 0.05 mm.

2.3. Diffraction measurements

Prior to data collection, suitable native crystals were soaked in a cryobuffer composed of mother liquor mixed with 20%(*v*/*v*) glycerol. Crystals were then mounted in a nylon loop and flash-cooled in liquid ethane at 120 K.

X-ray data were collected at 100 K on beamline ID14-4 at the European Synchrotron Radiation Facility (ESRF, Grenoble) with incident radiation at a wavelength of 0.934 Å and a crystal-to-detector distance of 220 mm. The diffraction spots were recorded on an ADSC-Q4 CCD detector with a 1.0° oscillation and a 5 or 15 s exposure per CCD image (for *C*2 and $P2_1$ crystals, respectively) over a range of 100°. Data were processed using *DENZO* and *SCALEPACK* (Otwinowski & Minor, 1996) and the indexed intensities were converted to structure factors using *TRUNCATE* from the *CCP*4 program suite (Collaborative Computational Project, Number 4, 1994) without any σ cutoff.

3. Results and discussion

Of the 296 crystallization conditions tested, three gave crystals. They were condition No. 9 from Molecular Dimensions Structure Screen 1 and condition No. 40 from Hampton Research Crystal Screen I [both containing 20%(*v*/*v*) PEG 4000, 20%(*v*/*v*) 2-propanol and 100 m*M* sodium citrate buffer pH 6.5] and condition No. 43 from Molecular Dimensions Structure Screen 2 [containing 35%(*v*/*v*) dioxan]. In the presence of dioxan, a few crystals grew in about one week (Fig. 1*a*). In the solution with PEG 4000 and 2-propanol only microcrystals grew, but their size could be optimized by modifying the crystallization conditions. Indeed, large crystals were obtained (Fig. 1*b*) by mixing 1 µl of reservoir solution containing 16%(*v*/*v*) PEG 4000, 16%(*v*/*v*) 2-propanol and 100 m*M* sodium citrate buffer pH 6.5 with 3 µl of a solution

Figure 2
Section v = 1/2 of the native Patterson map (u from 0 to 1/2 and w from 0 to 1) in space group $P2_1$, showing two symmetrically equivalent high peaks. These peaks correspond to a non-crystallographic translation described by the vector (x = 0.008, y = 0.500, z = 0.162) that relates two molecules in the asymmetric unit. Data were included in the resolution range 30.0–2.5 Å. The low-level cutoff is 3σ, with contour levels of 3σ.

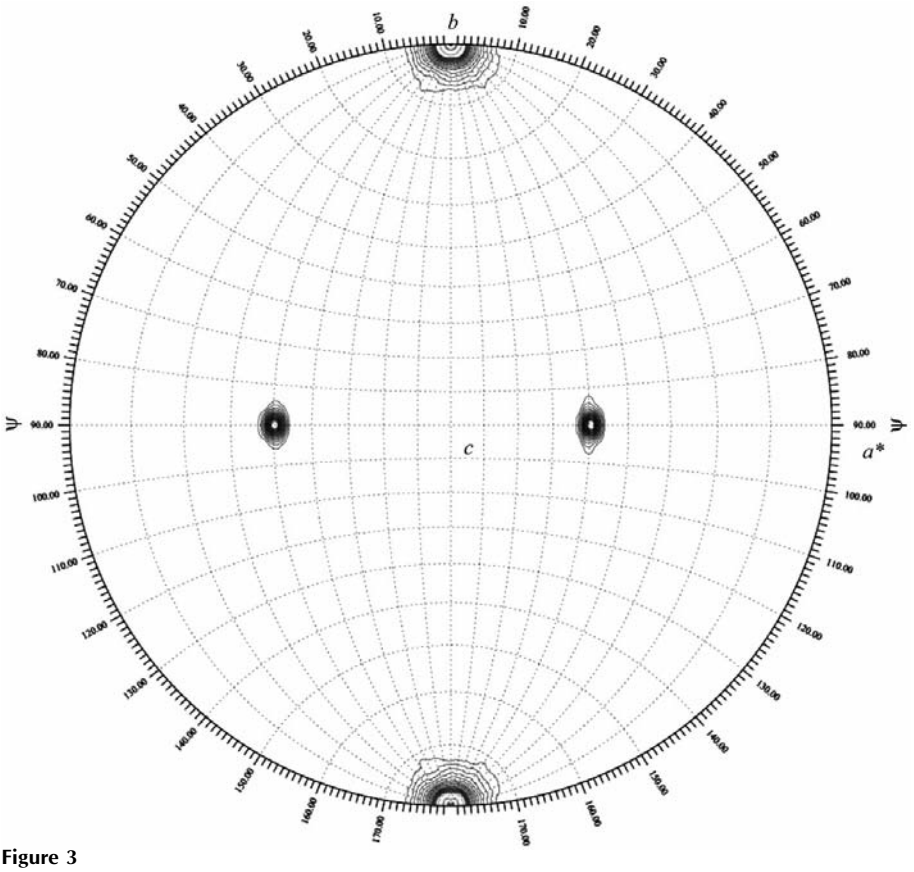

Figure 3
Stereographic projection of the $\kappa = 180^\circ$ section of a self-rotation function in space group $C2$ showing a non-crystallographic twofold axis. The crystallographic twofold axis is apparent in the two high-intensity (11.5σ) peaks at ($\varphi = 50$, $\psi = 90$, $\kappa = 180^\circ$) and ($\varphi = 140$, $\psi = 90$, $\kappa = 180^\circ$). Data were included between 10.0 and 3.0 Å with a 25 Å integration radius. The lowest contour level is at 2σ above the mean; the highest contour is at the maximum of the self-rotation function.

containing enzyme at 10 mg ml^{-1} in 20 m*M* Tris–HCl buffer pH 7.5.

AS-AR crystals grown in the presence of dioxan belong to a primitive monoclinic space group (Table 1). Systematic extinctions [$I/\sigma(I) < 3$] of $0k0$ (with $k = 2n + 1$) reflections indicate that the space group is $P2_1$. Since AS-AR is a homodimer with $M_r = 65\,000$, assumption of two dimers in the asymmetric unit leads to a packing density V_M of 3.63 Å^3 Da^{-1} and a solvent content of 66%. These values are in good agreement with those for other proteins (Matthews, 1968). Diffraction data were collected at a resolution limit of 3.0 Å using a synchrotron X-ray source (Table 1). A total of 107 806 reflections were recorded and reduced to 33 914 unique reflections. Overall, the R_{sym} was 9.0% on intensities ($R_{sym} = \sum |I - \langle I \rangle| / \sum I$) and the completeness was 90.3%. The results of self-rotation function calculations revealed only two high-intensity peaks at ($\varphi = 0$, $\psi = 0$, $\kappa = 180^\circ$) and ($\varphi = 0$, $\psi = 180$, $\kappa = 180^\circ$) that correspond to the crystallographic twofold axis (data not shown). A native Patterson map indicated two symmetrically related high-intensity peaks (28σ) characteristic of a non-crystallographic translation (Fig. 2).

The crystals of AS-AR obtained in the presence of PEG 4000 and 2-propanol belong to space group $C2$ (Table 1). Assuming one dimer in the asymmetric unit, the predicted packing density V_M is 1.94 Å^3 Da^{-1} and the solvent content is 36%. Diffraction data were collected to a resolution limit of 2.3 Å using a synchrotron X-ray source (Table 1). A total of 55 594 reflections were recorded and reduced to 21 186 unique reflections. Overall, the R_{sym} was 5.5% on intensities and the completeness was 95.7%. Calculation of a self-rotation function using the *GLRF* program (Tong & Rossmann, 1990) revealed two high-intensity peaks which correspond to a non-crystallographic twofold axis (Fig. 3). This result is in agreement with the presence of one dimer per asymmetric unit in the $C2$ crystals.

Determination of the crystal structure of AS-AR by molecular replacement using the available three-dimensional structures of the structurally and functionally related proteins *P. kodakaraensis* AspRS (Schmitt *et al.*, 1998; PDB code 1b8a) and *E. coli* AS-A (Nakatsu *et al.*, 1998; PDB code 12as) was not possible. AS-AR did not share significant sequence homology with *E. coli* AS-A and use of the structure of *P. kodakaraensis* AspRS, which shares 26% identity with AS-AR, did not allow solution of the structure. Therefore, our efforts are currently focused on the acquisition of phase information from selenomethionine-substituted protein and heavy-atom derivatives. We have produced crystals of the selenomethionine (SeMet) substituted protein. We are currently optimizing the crystallization conditions for SeMet crystals of AS-AR for use in the MAD method.

We are grateful to ESRF for granting access to the ID14 beamline and we thank the ESRF staff for assistance with data collection. We acknowledge Hampton Research, Molecular Dimensions Ltd and Decode Genetics for gifts of sparse-matrix kits in the frame of the EMBO Practical Workshop on crystallogenesis held in Strasbourg in September 2000 and Dr B. Lorber (IBMC, Strasbourg) for advice. This work was supported by Centre National de la Recherche Scientifique (CNRS), Université Louis Pasteur de Strasbourg and by grants from Association de la Recherche contre le Cancer (ARC) and from Centre National d'Etudes Spatiales (CNES). CC was the recipient of a CNES fellowships; HR and MB were recipients of a fellowship from Ministère de la Recherche et de la Technologie (MRT).

References

Becker, H. D. & Kern, D. (1998). *Proc. Natl Acad. Sci. USA*, **95**, 12832–12837.
Collaborative Computational Project, Number 4 (1994). *Acta Cryst.* D**50**, 760–763.
Jancarik, J. & Kim, S.-H. (1991). *J. Appl. Cryst.* **24**, 409–411.
Matthews, B. W. (1968). *J. Mol. Biol.* **33**, 491–497.
Nakatsu, T., Kato, H. & Oda, J. (1998). *Nature Struct. Biol.* **5**, 15–19.
Otwinowski, Z. & Minor, W. (1996). *Methods Enzymol.* **276**, 307–326.
Roy, H., Becker, H. D., Reinbolt, J. & Kern, D. (2003). *Proc. Natl Acad. Sci. USA*, **100**, 9837–9842.
Schmitt, E., Moulinier, L., Fujiwara, S., Imanaka, T., Thierry, J.-C. & Moras, D. (1998). *EMBO J.* **17**, 5227–5237.
Scofield, M. A., Lewis, W. S. & Schuster, S. M. (1990). *J. Mol. Biol.* **265**, 12895–12902.
Tong, L. & Rossmann, M. G. (1990). *Acta Cryst.* A**46**, 783–792.